

## Article

# Preparation, Optimization, and Characterization of Inclusion Complexes of *Cinnamomum longepaniculatum* Essential Oil in $\beta$ -Cyclodextrin

Yue Yan <sup>1,\*</sup>, Xin Zhao <sup>1</sup>, Chao Wang <sup>1</sup>, Qiong Fang <sup>1</sup>, Lu Zhong <sup>1</sup> and Qin Wei <sup>2,\*</sup>

<sup>1</sup> Faculty of Agriculture, Forestry and Food Engineering, Yibin University, Yibin 644001, China; 2019106011@yibinu.edu.cn (X.Z.); wang18181582933@163.com (C.W.); fangfang\_0717@163.com (Q.F.); zhonglu02022@163.com (L.Z.)

<sup>2</sup> Sichuan Province Engineering Technology Research Center of Oil Cinnamon, Yibin 610039, China

\* Correspondence: yue.yan@yibinu.edu.cn (Y.Y.); weiqin2001-67@163.com (Q.W.)

**Abstract:** *Cinnamomum longepaniculatum* essential oil (CLEO) possesses antibacterial, anti-inflammatory, and antioxidant activities. However, CLEO shows volatilization and poor solubility, which limits its application field. In this research, inclusion complexes of  $\beta$ -cyclodextrin ( $\beta$ -CD) with CLEO were produced, and its physicochemical properties were characterized. Response surface methodology was used to obtain optimum preparation conditions. A statistical model was generated to define the interactions among the selected variables. Results show that the optimal conditions were an H<sub>2</sub>O/ $\beta$ -CD ratio of 9.6:1 and a  $\beta$ -CD/CLEO ratio of 8:1, with the stirring temperature of 20 °C for the maximal encapsulation efficiency values. The physicochemical properties of CLEO/ $\beta$ -CD inclusion complexes (CLEO/ $\beta$ -CD-IC) were investigated. Fourier transform infrared spectroscopy showed that correlative characteristic bands of CLEO disappeared in the inclusion complex. X-ray diffraction presented different sharp peaks at the diffraction angle of CLEO/ $\beta$ -CD-IC. The thermogravimetric analysis demonstrated the thermal stability of CLEO was enhanced after encapsulation. Tiny aggregates with a smaller size of CLEO/ $\beta$ -CD-IC particles were observed by scanning electron microscopy. The comparison of  $\beta$ -CD, CLEO, and physical mixtures with CLEO/ $\beta$ -CD-IC confirmed the formation of inclusion complexes.

**Keywords:** *Cinnamomum longepaniculatum* essential oil; cyclodextrin; encapsulation; response surface methodology



**Citation:** Yan, Y.; Zhao, X.; Wang, C.; Fang, Q.; Zhong, L.; Wei, Q. Preparation, Optimization, and Characterization of Inclusion Complexes of *Cinnamomum longepaniculatum* Essential Oil in  $\beta$ -Cyclodextrin. *Sustainability* **2022**, *14*, 9513. <https://doi.org/10.3390/su14159513>

Academic Editors: Juan Francisco García Martín, Chao Hui Feng and Yoshio Makino

Received: 13 June 2022

Accepted: 29 July 2022

Published: 3 August 2022

**Publisher's Note:** MDPI stays neutral with regard to jurisdictional claims in published maps and institutional affiliations.



**Copyright:** © 2022 by the authors. Licensee MDPI, Basel, Switzerland. This article is an open access article distributed under the terms and conditions of the Creative Commons Attribution (CC BY) license (<https://creativecommons.org/licenses/by/4.0/>).

## 1. Introduction

The *Cinnamomum* genus tree *Cinnamomum longepaniculatum* (Gamble) N. Chao ex H. W. Li (*C. longepaniculatum*) is an endemic species in China [1]. Many parts of *C. longepaniculatum* contain volatile essential oil, which provides raw materials for the essence, food, medicine, cosmetics, and other chemical industries. The economic value of *C. longepaniculatum* is abundant essential oil content in the leaves and twigs, approximately 3.8 to 4.5%. The main ingredient of *C. longepaniculatum* essential oil (CLEO) includes 1,8-cineole,  $\alpha$ -terpineol, terpinen-4-ol,  $\alpha$ -pinene,  $\alpha$ -phellandrene,  $\gamma$ -terpinene, and  $\beta$ -pinene (Figure 1) [2,3].

Various chemical constituents of *C. longepaniculatum* essential oil were inferred and verified its multiple biological activities by previous studies. It has an excellent antibacterial effect and anti-inflammatory actions by in vitro and in vivo experiments. Moreover, anti-cancer, analgesic, anthelmintic, and antioxidant effects were also confirmed [4,5]. Terpenes and sterols of CLEO as traditional pharmaceuticals or food additives were discovered in many medicinal and aromatic plants.

CLEO, as an essential oil, is sensitive and readily decomposed by heating and exposure to light and oxygen. Degradation of essential oil accompanies chemical group modifications

and can cause color changes, unpleasant odor, and decreased activity [6]. Furthermore, the physical properties of essential oil, such as low water solubility and volatilization, limit its application potential in more fields [7]. In order to protect essential oil and improve physicochemical properties, it can be encapsulated into host molecules cyclodextrins (CDs).

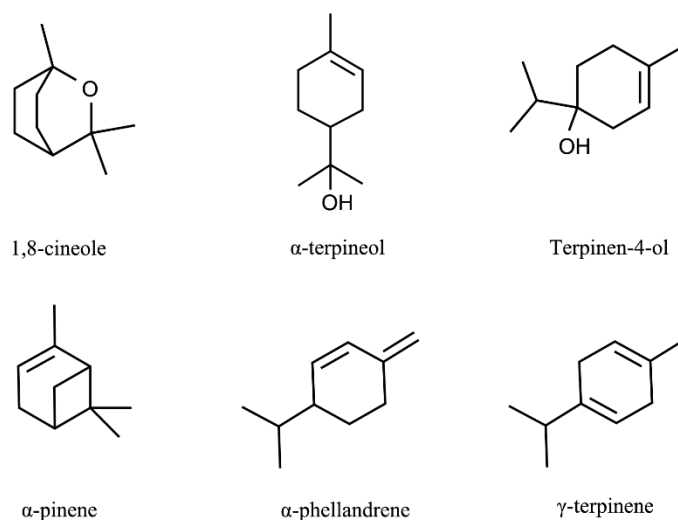


**Figure 1.** Chemical structures of representative major compounds for *C. longepaniculatum* essential oil.

CDs are cyclic oligosaccharides consisting of D-glucopyranose units and connected by  $\alpha$ -1,4 glucosidic bond, issued from starch enzymatic hydrolysis. CDs have truncated cone shapes and hydrophobic cavities. Hydroxyl groups are faced outwards, while hydrogen atoms and glycosidic oxygen bridges rotate inwards to form lipophilicity [8]. Geometric hydrophobic compounds can be partly or fully enveloped in cavity interiors [9]. The amount of glucose units decides the cavity size and the ability to accommodate hydrophobic guest molecules [10]. CDs are non-poisonous agents and have been utilized as wall materials to control the core materials' release and prolong their shelf life. Frequently-used inclusion material was  $\beta$ -CD, with advantages such as suitable cavity size, ease of production, low oral poisonousness, and easy-to-form inclusion complexes with organic solvents [11].  $\beta$ -CD can be used to encapsulate the essential oil due to the 0.6–0.8 nm cavity size suitable for essential oil compounds (relative molecular mass from 80 to 250) [12]. When  $\beta$ -CD and guest compounds form inclusion complexes, physicochemical properties of the complex can be changed compared with guest compounds, including improved solubility, stability, and bioavailability; meanwhile, reduced adverse reactions. Therefore, in pharmaceutical, agriculture, food, and cosmetic industries,  $\beta$ -CD is utilized to manufacture inclusion complexes [13–17]. Several studies have demonstrated the process and performance of inclusion complexes based on  $\beta$ -CD and various essential oil [18–20].

Response surface methodology (RSM), as a multivariate statistical technique, is applied for optimizing complex processes [21–24]. Although previous studies have studied the preparation of CLEO inclusion complexes, the application of RSM to the encapsulation and physicochemical characterization of inclusion complexes has not been exploited [25]. The main purpose of this research is to produce *C. longepaniculatum* essential oil/ $\beta$ -cyclodextrin inclusion complexes (CLEO/ $\beta$ -CD-IC), establish an optimum process parameter condition, and estimate the physicochemical characterization of products.

## 2. Materials and Methods

### 2.1. Materials

*C. longepaniculatum* volatile essential oil (CLEO), extracted from *C. longepaniculatum* leaf by hydrodistillation method, was provided by Shiping Spice Co., Ltd. (Yibin, China),  $\beta$ -CD was purchased from Sinopharm Chemical Reagent Co., Ltd. (Shanghai, China). Ethanol

was analytical grade and obtained from KeLong Chemicals Co., Ltd. (Chengdu, China). Other reagents were analytical grade.

## 2.2. Preparation of Inclusion Complexes

CLEO/ $\beta$ -CD-IC was produced by the saturated aqueous solution method by the literature with slight modifications [26]. Appropriate quality of  $\beta$ -CD was deliquesced in preheated deionized water to form the  $\beta$ -CD saturated solution. A specified volume of CLEO ethanolic solution (1:10, *v/v*) was tardily introduced into the  $\beta$ -CD solution. The mixed solution was stirred on a thermostatic agitator at a particular temperature. After stirring for a preset time, the solution was cooled down and stored at 4 °C for 24 h. The sediments were vacuum percolated, and then powders were collected and put into the hot air circulating oven at 60 °C until dry at a constant weight.

To prepare physical mixtures,  $\beta$ -CD and CLEO were homogenized in the mortar and pestle at room temperature [11]. The mixtures were placed in a hermetically sealed glass for further use.

## 2.3. Encapsulation Efficiency (EE) and Loading Efficiency (LE)

The total essential oil in CLEO/ $\beta$ -CD-IC was distilled through the Clevenger-type hydrodistillation method. Obtained inclusion complexes were added into deionized water and distilled for 2 h. The volatile oil layer divided and located in the arm of the Clevenger's units. Subsequently, the weight of the volatile oil was determined.

The EE and LE were calculated by the following equation, respectively.

$$EE (\%) = \frac{M_E}{M_I} \times 100\% \quad (1)$$

$$LE (\%) = \frac{M_E}{M_T} \times 100\% \quad (2)$$

where  $M_E$  represented the mass of CLEO encapsulated,  $M_I$  was the mass of CLEO added initially, and  $M_T$  referred to the total mass of CLEO/ $\beta$ -CD-IC.

## 2.4. The Response Surface Methodology

### 2.4.1. Single-Factor Experiments

Before designing the response surface parameter, single-factor experiments were carried out to decide the appropriate range of various factors [27]. The ranges of independent variables were as follows: ratios of H<sub>2</sub>O to  $\beta$ -CD (5:1, 10:1, 15:1, 20:1, 25:1 mL/g), stirring time (0.5, 1, 1.5, 2, 2.5 h), ratios of  $\beta$ -CD to CLEO (4:1, 6:1, 8:1, 10:1, 12:1 g/mL) and stirring temperature (20, 30, 40, 50, 60 °C) [28]. The effect of each factor was determined by changing it in defined ranges while all other factors were constant, where the H<sub>2</sub>O/ $\beta$ -CD ratio was 5:1, stirring time was 1 h,  $\beta$ -CD/CLEO ratio was 10:1, and stirring temperature was 20 °C; each experiment was repeated three times.

### 2.4.2. Optimization of Experimental Design

RSM combined with the Box–Behnken design was carried out for optimization experiments on the encapsulation efficiency (*Y*) as the response variable [29]. According to data of the single-factor tests, three factors, including CLEO/ $\beta$ -CD ratio (*A*), stirring temperature (*B*), and stirring time (*C*), were selected as variables to conduct runs of RSM. Three levels of variates were confirmed on the basis of preliminary tests and coded as −1, 0, and 1 [30]. Factors codes and levels are shown in Table 1.

**Table 1.** Range of independent variables in RSM.

Variable	Symbol	Level of Variation		
		−1	0	1
H <sub>2</sub> O/β-CD ratio (g/mL)	A	5:1	10:1	15:1
β-CD/CLEO ratio (g/mL)	B	6:1	8:1	10:1
Stirring temperature (°C)	C	20	30	40

The experimental results were fitted to a second-order polynomial formula to survey the effects of autonomous factors and the correlation with the response variable.

$$Y = \alpha_0 + \alpha_1 A + \alpha_2 B + \alpha_3 C + \alpha_{11} A^2 + \alpha_{22} B^2 + \alpha_{33} C^2 + \alpha_{12} AB + \alpha_{13} AC + \alpha_{23} BC \quad (3)$$

where Y represented the response variable;  $\alpha_0$  was the constant;  $\alpha_1$ – $\alpha_3$  were linear coefficients;  $\alpha_{11}$ ,  $\alpha_{22}$ , and  $\alpha_{33}$  were quadratic coefficients; and  $\alpha_{12}$ ,  $\alpha_{13}$ , and  $\alpha_{23}$  were interactive coefficients.

### 2.5. Fourier Transform Infrared (FTIR) Spectroscopy

FTIR spectra of β-CD, CLEO, physical mixtures, and CLEO/β-CD-IC were obtained on an FTIR spectrometer (Nicolet iS 5, Thermo Scientific, Waltham, MA, USA) to detect the variation in typical peaks of β-CD after the encapsulation. Spectra were performed at the region of 4000 to 400 cm<sup>−1</sup> with 32 scans at an optical resolution of 4 cm<sup>−1</sup>.

### 2.6. X-ray Diffractogram (XRD) Analysis

The XRD analysis was performed by an X-ray diffractometer (Ultima IV, Rigaku, Tokyo, Japan). The operation was processed with Cu Kα radiation at 40 KV voltage and of 30 mA current. Each scan was performed in a 2θ angle range from 5° to 60° with a step size of 0.02° at the scanning speed of 5°/min.

### 2.7. Thermogravimetry/Derivative Thermogravimetry (TG/DTG) Analysis

The thermal stability of β-CD, CLEO, physical mixtures, and CLEO/β-CD-IC were measured on a thermogravimetric analyzer (TQ5000IR, TA Instruments, New Castle, DE, USA). Each sample was heated from 30 °C up to 300 °C, with a heating rate of 10 °C/min under a 50 mL/min flow nitrogen atmosphere. DTG results of respective targets were calculated by the first derivative of weight (%) versus time (min).

### 2.8. Differential Scanning Calorimetry (DSC)

A differential scanning calorimeter (DSC 214, NETZSCH, Selb, Germany) was used to conduct DSC thermograms of the samples. In this process, the temperature range was performed between 30 °C and 500 °C, and the heating rate was increased by 10 °C/min with a continuous nitrogen flow.

### 2.9. Morphological Examination

The morphological structure of β-CD, physical mixtures, and CLEO/β-CD-IC were evaluated using a scanning electron microscope (SEM, JSM-7200F, JEOL, Tokyo, Japan) at a voltage of 5 kV and different levels of magnification from 1000× to 5000×. Each sample was covered with thin golden layer before scanning to ensure complete conductivity.

### 2.10. Statistical Analysis

Results were presented as the average and standard deviation values. Statistical analysis was executed by one-way ANOVA using IBM SPSS Statistics 22 (IBM Co., New York, NY, USA), followed by the Bonferroni post hoc test for specific comparisons. *p* values < 0.05 were deemed to be significant difference. Design Expert 12 (Stat-Ease Inc., Minneapolis, MN, USA) was used in the response surface tests design, mathematical modeling, and optimization of the data.

### 3. Results and Discussion

#### 3.1. Effects of Single Factors

Single factor results certified that the H<sub>2</sub>O/ $\beta$ -CD ratio,  $\beta$ -CD/CLEO ratio, and stirring temperature significantly affected the EE and LE. Figure 2a shows that different H<sub>2</sub>O/ $\beta$ -CD ratios had an effect on the EE and LE. The EE improved with the rising concentration of the  $\beta$ -CD solution from H<sub>2</sub>O/ $\beta$ -CD ratio 25:1 to 10:1 and was highest at 10:1 ratio. Then, the EE decreased at 5:1. Meanwhile, the LE expressed a similar trend and was highest at a 10:1 ratio. It demonstrated that water-occupied  $\beta$ -CD non-polar groups were easily replaced by CLEO molecules and caused a high embedding rate at a certain concentration of host molecules solution.

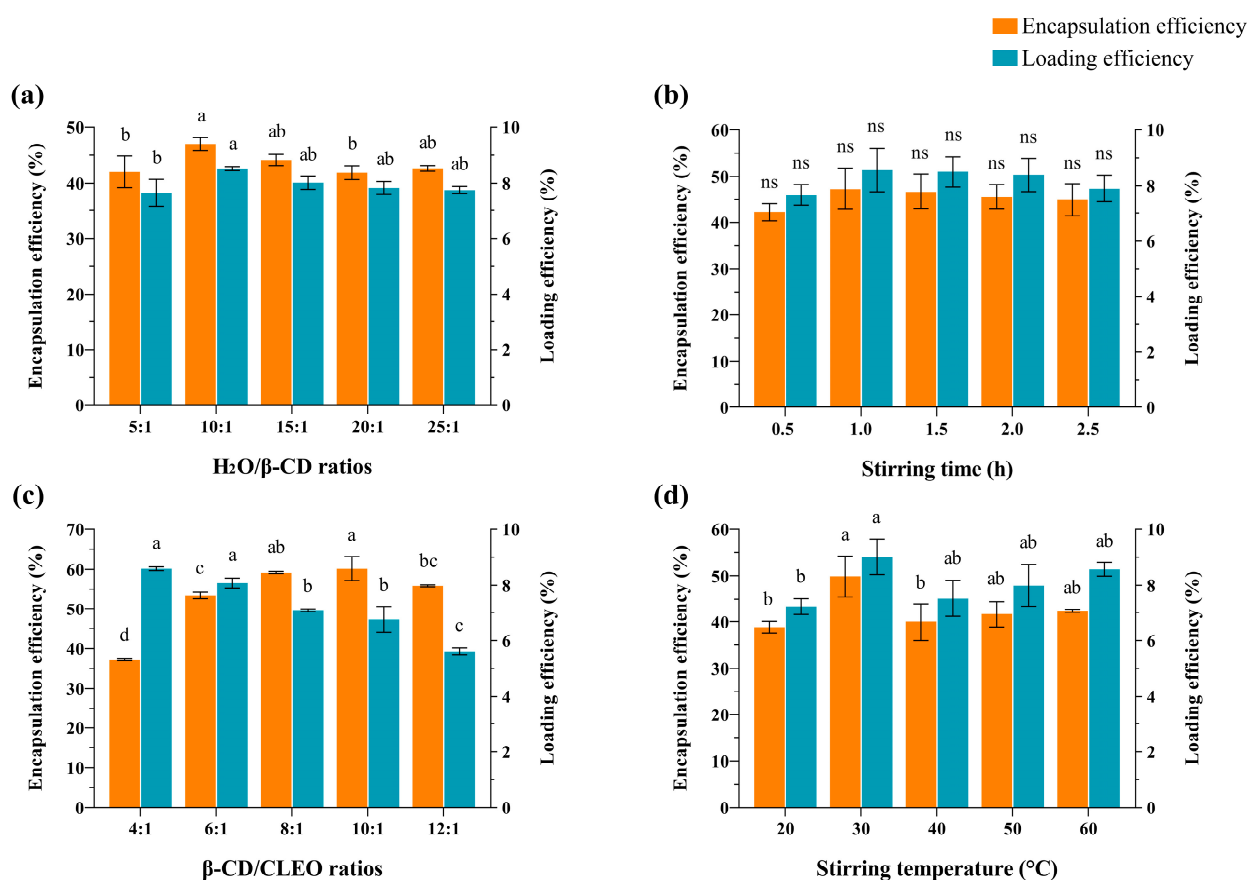


**Figure 2.** Effect of independent variable on the EE and LE of CLEO/ $\beta$ -CD-IC. H<sub>2</sub>O/ $\beta$ -CD ratios (a); stirring time (b);  $\beta$ -CD/CLEO ratios (c); stirring temperature (d). Note: Values labelled by diverse letters (a–c) means significant difference ( $p < 0.05$ ); ns indicates not significant.

Figure 2b displays that the impact of different times on the EE and LE was not significant. After a definite stirring time, the encapsulation and disassembly rate achieved balance. With the extension of time, volatilization and degradation of essential oil may be more serious, making the EE and LE steady or even decline.

Figure 2c shows  $\beta$ -CD/CLEO ratio had a dramatic influence on the EE and LE. As the  $\beta$ -CD/CLEO ratio increased, the EE continuously improved until the 10:1 ratio. However, LE was significantly reduced when  $\beta$ -CD/CLEO ratio was more than 8:1. This is determined by the molecular structure of  $\beta$ -CD, where seven glucose residues determine the size of its hydrophobic inner cavity diameter, which can only hold a limited number of guest molecules. Thus, the EE can increase based on an adequate amount of wall materials. Nevertheless, when most cyclodextrin molecules were filled with essential oil, with the increase in cyclodextrin content, the EE could not be improved and accompanied LE visibly decreased. On the other hand, excessive CLEO could lead to an inadequate envelope, with

CLEO adhering to the external  $\beta$ -CD and causing a decrease in the EE and LE. In other inclusion complexes studies, the concentrated orange oils/ $\beta$ -CD ratio of 12:88 showed a greater encapsulation capacity [31]. Retention of cinnamon essential oil attained the peak at the essential oil to the  $\beta$ -CD ratio of 10:90 [32].

Figure 2d reveals the EE was not continuously added with increasing stirring temperature. The higher EE did not occur at a high temperature exceeding 40 °C. The stirring temperature influenced the stability of CLEO/ $\beta$ -CD-IC. While the temperature increases to an extremely high degree, the disorder of molecules movement may occur, resulting in a partially disintegrate of the inclusion complexes. In addition, more volatilization of CLEO occurs at high temperatures, which reduces the EE [29].

### 3.2. Optimization of CLEO/ $\beta$ -CD-IC

Single-factor tests indicated that H<sub>2</sub>O/ $\beta$ -CD ratios,  $\beta$ -CD/CLEO ratio, and stirring temperature affected the EE. In order to optimize the three variables for preparing CLEO/ $\beta$ -CD-IC, RSM with a BBD design was applied based on three factors and three levels on the basis of single-factor trial results. A total of 17 measurements were performed. The EE ranged from 34.56% to 67.98%, as shown in Table 2.

**Table 2.** Box–Behnken design scheme and the response.

Runs	A	B	C	Y
	H <sub>2</sub> O/ $\beta$ -CD Ratio (mL/g)	$\beta$ -CD/CLEO Ratio (g/mL)	Stirring Temperature (°C)	Encapsulation Efficiency (%)
1	5	4	30	36.10
2	15	6	20	52.65
3	15	8	30	61.27
4	10	8	20	67.98
5	10	8	40	63.59
6	10	6	30	54.02
7	10	6	30	52.84
8	5	8	30	63.09
9	15	4	30	36.07
10	10	6	30	54.58
11	10	6	30	54.17
12	5	6	40	48.30
13	10	4	20	34.56
14	10	4	40	37.19
15	5	6	20	52.92
16	15	6	40	45.42
17	10	6	30	52.16

A quadratic model was elected for regression analysis, and the resulting model fitted to a second-order polynomial regression formula was represented following:

$$Y = 53.55 - 0.63A + 14.00B - 1.70C - 2.71A^2 - 1.71B^2 - 1.02C^2 - 0.45AB - 0.65AC - 1.75BC \quad (4)$$

As shown in Table 3, the ANOVA presents that the model was significant ( $p < 0.05$ ), and simultaneously a lack of fit was non-significant ( $p > 0.05$ ). This suggested that the variables in the model can explain the experimental variation of the EE. In this model, the R<sup>2</sup> was 0.9856, and the adjusted R<sup>2</sup> was 0.967, manifesting relevance existed between the observed and predicted values.

The most significant effect was the linear term of  $\beta$ -CD/CLEO ratio (B) ( $p < 0.01$ ), and the linear term of stirring temperature (C) was also significant ( $p < 0.05$ ). Quadratic terms of A presented a significant influence ( $p < 0.05$ ); however, quadratic terms of B and C were not significant.

**Table 3.** ANOVA for the EE response of preparation of CLEO/ $\beta$ -CD-IC.

Variance Origin	Sum of Squares	df	Mean Square	F-Value	p-Value	Significance
Model	1661.61	9	184.62	53.15	<0.0001	significant
A	3.13	1	3.13	0.8996	0.3745	-
B	1568.28	1	1568.28	451.46	<0.0001	significant
C	23.15	1	23.15	6.67	0.0364	significant
A <sup>2</sup>	31.03	1	31.03	8.93	0.0203	significant
B <sup>2</sup>	12.27	1	12.27	3.53	0.1023	-
C <sup>2</sup>	4.35	1	4.35	1.25	0.2998	-
AB	0.8010	1	0.8010	0.2306	0.6457	-
AC	1.70	1	1.70	0.4902	0.5064	-
BC	12.32	1	12.32	3.55	0.1017	-
Residual	24.32	7	3.47	-	-	-
Lack of Fit	20.21	3	6.74	6.57	0.0503	not significant
Pure Error	4.10	4	1.03	-	-	-
Cor Total	1685.93	16	-	-	-	-
R <sup>2</sup>	0.9856	-	-	-	-	-
Adjusted R <sup>2</sup>	0.9670	-	-	-	-	significant
Model	1661.61	9	184.62	53.15	<0.0001	significant

Note: A: H<sub>2</sub>O/ $\beta$ -CD ratio, B:  $\beta$ -CD/CLEO ratio, C: stirring temperature. A<sup>2</sup>, B<sup>2</sup>, and C<sup>2</sup> mean square of A, B, and C.

3D response surface plots were applied to visualize the interaction between two factors and the maximum EE on each variable. Figure 3 displays two variables kept constant and another variable altered in a specified scope. In Figure 3a, when the temperature was fastened at the center point (30 °C), the EE was increased by improving the  $\beta$ -CD/CLEO ratio from 4:1 to 8:1 and reached the maximum value at 8:1. Figure 3b indicates that keeping  $\beta$ -CD/CLEO ratio at 6:1, the maximum with the highest desirability lies towards the intermediate values of H<sub>2</sub>O/ $\beta$ -CD ratio. When at a higher temperature, volatilization of CLEO will lead to a decrease in EE [33]. The contour plots are elliptical, suggesting that the two factors have some interaction.

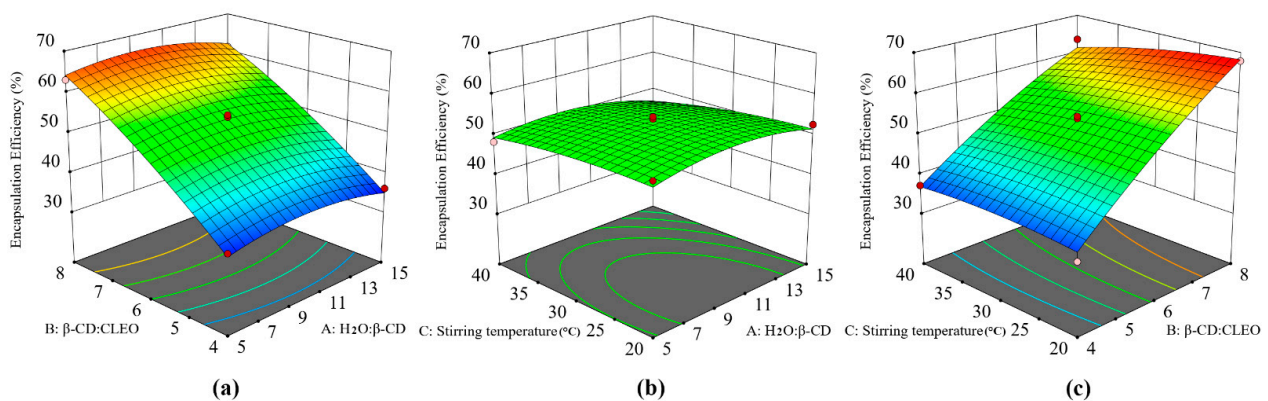


**Figure 3.** Response surface plots revealing effects of H<sub>2</sub>O/ $\beta$ -CD ratio (a),  $\beta$ -CD/CLEO ratio (b), and stirring temperature (c) on the EE.

Verification tests were applied to validate the recommendatory optimized criteria from the derivation of RSM. The optimum procedure for the EE was designed at an H<sub>2</sub>O/ $\beta$ -CD ratio of 9.614:1, a  $\beta$ -CD/CLEO ratio of 8:1, and a stirring temperature of 20 °C, which predicted an EE of 68.304%. The optimal conditions were modified according to the actual situation as follows: H<sub>2</sub>O/ $\beta$ -CD ratio of 9.6:1,  $\beta$ -CD/CLEO ratio of 8:1, and stirring temperature of 20 °C. The observed results were 68.31%  $\pm$  1.13%, comparable with the predictand. This indicated a superior correlation between predictand and practical data

by the regression model. Consequently, the preparation conditions obtained by RSM were verified and can be used to predict the EE effectually.

### 3.3. FTIR Spectroscopy

FTIR technique allows the recognition of vibration motion and rotation motion of bonds in molecules. Therefore, FTIR is widely utilized to illustrate the guest molecules and cyclodextrins during the inclusion process through characteristic bands of guest and host molecules shifting, decreasing, enlarging, or disappearing [34]. The formation process of inclusion complexes between guest and host molecules relates to chemical interaction through the hydrophobic interactions and H-bonding forces in the internal cavity of the host molecules. For this reason, it can serve to demonstrate the complex formation between CLEO and  $\beta$ -CD. In Figure 4, the representative bands of the CLEO,  $\beta$ -CD, corresponding physical mixtures, and CLEO/ $\beta$ -CD-IC are displayed.

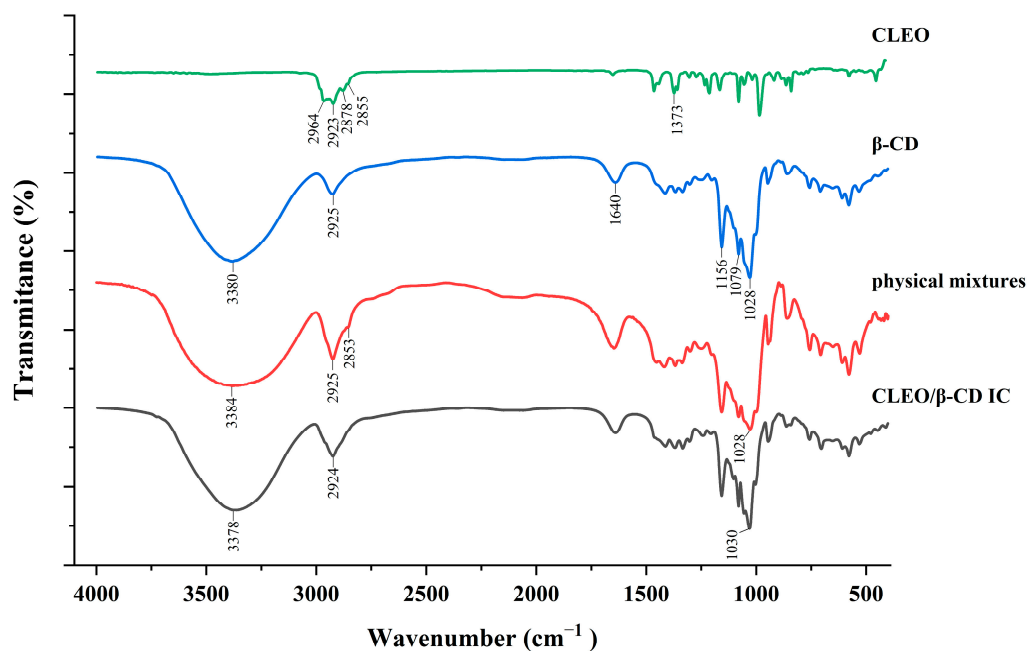


**Figure 4.** FTIR spectra of CLEO,  $\beta$ -CD, physical mixtures and CLEO/ $\beta$ -CD-IC.

The FTIR spectrum of CLEO illustrates representative bands following: stretching vibration of the methyl ( $\text{CH}_3$ ) groups at  $2964\text{ cm}^{-1}$  and  $2878\text{ cm}^{-1}$ , stretching vibration of methylene ( $\text{CH}_2$ ) groups at  $2923\text{ cm}^{-1}$  and  $2853\text{ cm}^{-1}$ ,  $\text{CH}_3$  groups bending vibration at  $1373\text{ cm}^{-1}$  [35].

The infrared spectrum of  $\beta$ -CD depicts the broad bands of the stretching vibration of the O-H group at  $3380\text{ cm}^{-1}$ . While other bands can also be related:  $2925\text{ cm}^{-1}$  for  $\text{CH}_2$  groups stretching vibration,  $1640\text{ cm}^{-1}$  for H-O-H bending vibration,  $1156\text{ cm}^{-1}$  for C-O-C stretching vibration,  $1079\text{ cm}^{-1}$  for C-C stretching vibrations, and  $1028\text{ cm}^{-1}$  for C-O stretching vibration. Similar results can be found reported previously [9,36].

The physical mixture spectrum presents the characteristic bands of  $\beta$ -CD:  $3384\text{ cm}^{-1}$  (OH),  $2925\text{ cm}^{-1}$  ( $\text{CH}_2$ ), and  $1028\text{ cm}^{-1}$  (C-O). Moreover, the representative bands of CLEO,  $2853\text{ cm}^{-1}$  ( $\text{CH}_2$ ), are also observed, suggesting CLEO was not covered up and did not interact with  $\beta$ -CD by being mixed physically.

The spectrum of the CLEO/ $\beta$ -CD-IC is practically completely derived from wide and intense bands of  $\beta$ -CD [37]. The representative wavenumbers of O-H stretching vibration from  $\beta$ -CD decreased, while the wavenumber values of C-O stretching vibrations were slightly increased after encapsulation. This can be interpreted as hydrophobic interaction between essential oil components in CLEO has been partially displaced by interactions between essential oil molecules and  $\beta$ -CD cavity, and hydrogen bonds were also established

between hydroxyl groups of essential oil with cyclodextrins, which altered the characteristic bands after complexation. The characteristic absorption bands of CLEO at  $2964\text{ cm}^{-1}$ ,  $2878\text{ cm}^{-1}$ ,  $2923\text{ cm}^{-1}$ , and  $2853\text{ cm}^{-1}$  vanished from the spectrum of the CLEO/ $\beta$ -CD-IC since the active CLEO was incorporated into the  $\beta$ -CD cavity, forming a strong physical cross-link, limiting the vibrations of aforementioned groups. Similar results for encapsulation can be found in the literature [38].

### 3.4. XRD Analysis

The crystalline state of the samples can be reflected by X-ray diffraction analysis. Figure 5 represents the XRD patterns of  $\beta$ -CD, physical mixtures, and CLEO/ $\beta$ -CD-IC. The  $\beta$ -CD crystalline profile exhibits intense and narrow peaks. The main sharp diffraction peaks were between  $9^\circ$  and  $27^\circ$  at  $2\theta$  values, and less intense peaks were located in the range of  $32^\circ$  to  $44^\circ$  [39]. No visible difference was perceived in the diffractograms of the physical mixtures compared with  $\beta$ -CD, demonstrating a novel phase was not established, which proved the inclusion complexes can not be acquired by a primitively physical blend of the raw materials. Conversely, in comparison to  $\beta$ -CD, the diffraction maximum of CLEO/ $\beta$ -CD-IC was obviously weakened or disappeared at  $9.1^\circ$ ,  $10.7^\circ$ ,  $12.6^\circ$ ,  $22.8^\circ$ , and  $27.1^\circ$ , while peaks of  $7.2^\circ$ ,  $14.5^\circ$ ,  $15.2^\circ$ ,  $17.5^\circ$  emerged. The diffractogram demonstrated a new crystalline structure, which may be issued from CLEO entrapped into the cavity interior of  $\beta$ -CD. Qualitatively, the partial diffraction peaks approximate to  $\beta$ -CD revealed CLEO/ $\beta$ -CD-IC have a higher proportion of  $\beta$ -CD participating in the complexation and demined the interaction. The above results supported that CLEO and  $\beta$ -CD formed inclusion complexes in solid-phase with unique characteristics.

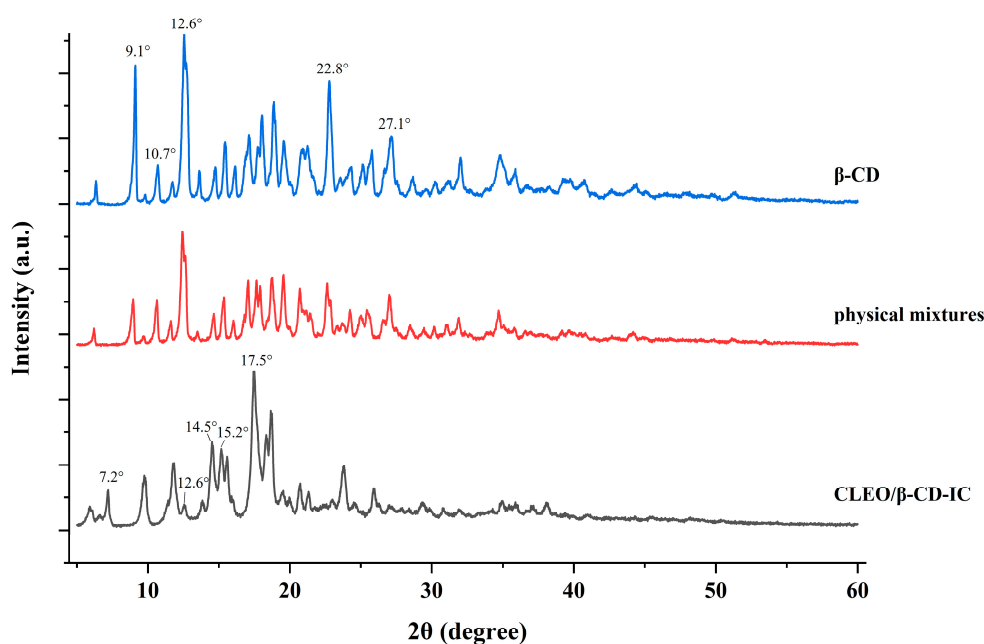


**Figure 5.** XRD patterns of  $\beta$ -CD, physical mixtures, and CLEO/ $\beta$ -CD-IC.

### 3.5. TG/DTG and DSC

Thermogravimetric analysis has been employed as a proven technique for evaluating the guest molecule interacting with host materials in a kinetic control regime. The TG/DTG profiles of  $\beta$ -CD, CLEO, physical mixtures, and CLEO/ $\beta$ -CD-IC were exhibited in Figure 6a,b. The thermal decomposition of  $\beta$ -CD exited two degradation stages [40]. The first stage at the range of  $50$  to  $105^\circ\text{C}$  was the evaporation of the water-binding  $\beta$ -CD, while the second stage was above  $310^\circ\text{C}$  due to molecular main chain decomposition. The TG curves of CLEO showed an obvious mass loss from beginning to  $130^\circ\text{C}$ , correlated with the volatilization of CLEO. For the physical mixtures thermograms, two weight loss

steps were located at 30 to 110 °C and 320 to 360 °C. The former presented evaporation of water in  $\beta$ -CD and high volatilization of essential oil, while the latter presented degradation of  $\beta$ -CD. The TG curves of CLEO/ $\beta$ -CD-IC were inconsistent with those of  $\beta$ -CD or physical mixtures. The thermograms revealed an attenuated weight loss under 310 °C. This may be interpreted as the reduction of the proportion of water-binding  $\beta$ -CD, which was partially replaced by CLEO-based appropriate hydrophobic ligands. A protracted weight loss of CLEO/ $\beta$ -CD-IC was also related to the evaporation of endogenic CLEO, which continuously heated to 310 °C. Since the decomposition temperature of CLEO/ $\beta$ -CD-IC exceeds those of  $\beta$ -CD and physical mixtures, it demonstrated forming inclusion complexes increased the thermal stability of CLEO.

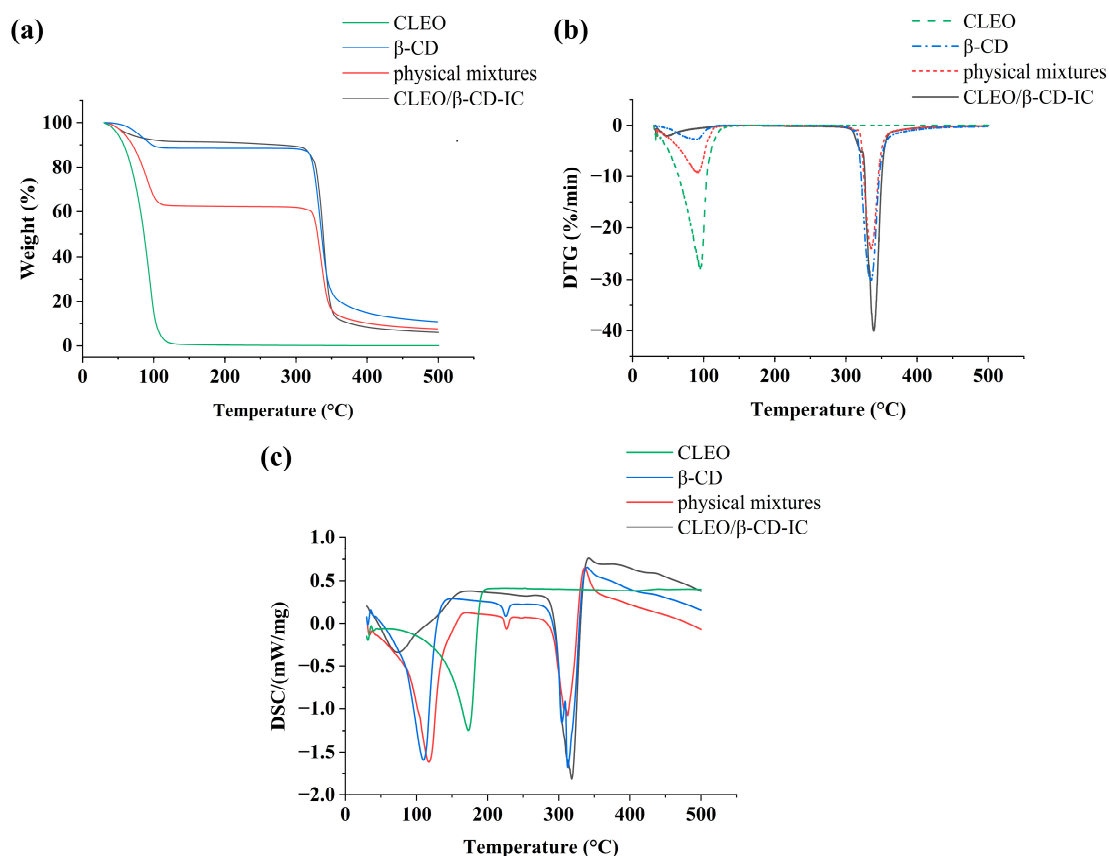


**Figure 6.** Thermogravimetry curves (a), DTG curves (b) and DSC thermogram (c) of CLEO,  $\beta$ -CD, physical mixtures and CLEO/ $\beta$ -CD-IC.

DSC was also utilized to investigate the thermal characteristics of each sample, and the results are exhibited in Figure 6c. The DSC curve of CLEO indicated a wide endothermic peak from 140.1 °C to 188.4 °C, corresponding to its decomposition process. For the thermogram of  $\beta$ -CD, the endothermic peak of 73.3–127.4 °C is concerned with water loss in the cavity interior of  $\beta$ -CD. The semblable DSC curve of physical mixtures manifested that disengaged  $\beta$ -CD subsist in the physical mixtures. After encapsulation, changes in the DSC curve were discovered in the thermograms of CLEO/ $\beta$ -CD-IC. The shift of the endothermic peak and decline of the area in the inclusion complexes represented the disorder of the water inside the  $\beta$ -CD cavity [41]. Strikingly, no typical endothermic peak of CLEO appeared in the CLEO/ $\beta$ -CD-IC curve, confirming that CLEO had been defended in the hydrophobic cavity of  $\beta$ -CD. Therefore, combined with the findings of FTIR and XRD, it was demonstrated the inclusion complexes formed successfully [42].

### 3.6. Morphological Detection

The topography of  $\beta$ -CD, physical mixtures, and CLEO/ $\beta$ -CD-IC were compared through scanning by SEM to acquire microscopic pictures (Figure 7).  $\beta$ -CD particles displayed amorphous, irregular crystals with different sizes and comparative dense structures [43]. The morphology of physical mixtures did not show remarkable variation compared to  $\beta$ -CD on shapes and sizes, certifying no interaction with each other. In contrast, the SEM images of CLEO/ $\beta$ -CD-IC were unlike those of  $\beta$ -CD and physical mixtures. CLEO/ $\beta$ -CD-IC particles appeared in the form of tiny aggregates with smaller sizes and altered shapes. In the inclusion complexes, typical structures of cyclodextrins disappeared.

In other works of literature, *Croton rhamnifolioides* essential oil [44], *Lippia pedunculosa* essential oil [45], and *Exocarpium Citri Grandis* essential oil [6] complexed with cyclodextrins, respectively, the morphology and particle sizes of inclusion complexes were transformed compared to pure  $\beta$ -CD. Multiple morphologies of various inclusion complexes can be observed, which may be based on the admitting ability of the  $\beta$ -CD cavity on various guest molecules to encapsulation. This behavior revealed the interaction between essential oil and  $\beta$ -CD and the accomplishment of encapsulation.

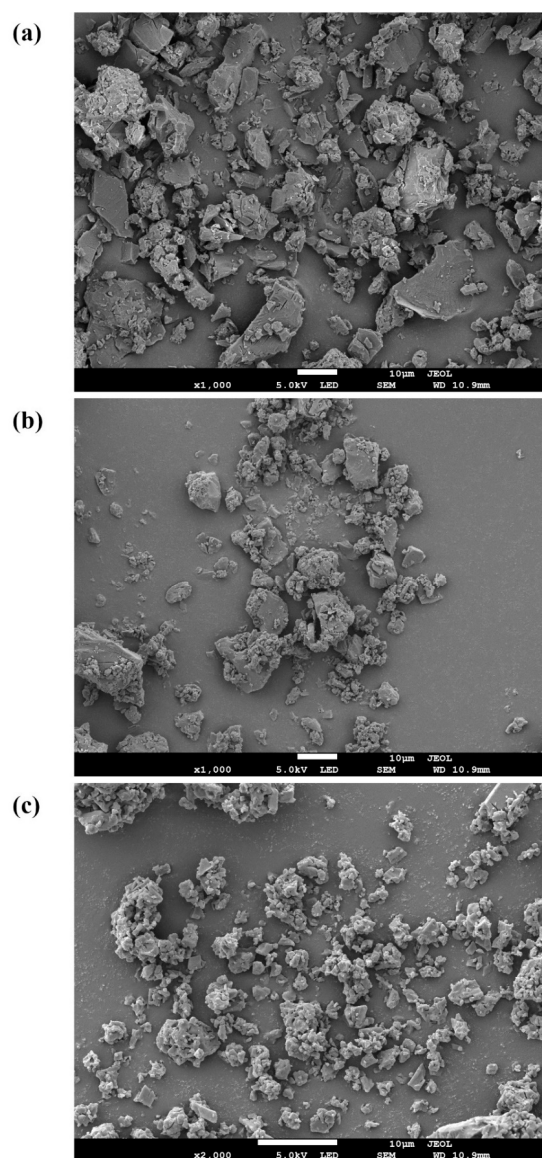


Figure 7. SEM micrographs of  $\beta$ -CD  $\times$  1.0 k (a), physical mixtures  $\times$  1.0 k (b), CLEO/ $\beta$ -CD-IC  $\times$  2.0 k (c).

#### 4. Conclusions

The inclusion complexes of CLEO with  $\beta$ -CD were produced using the saturated solution method. The quadratic model was established for the EE, and the following optimal procedure parameters were acquired by response surface methodology: 9.6:1 of H<sub>2</sub>O/ $\beta$ -CD ratio, 8:1 of  $\beta$ -CD/CLEO ratio, 20 °C of stirring temperature. The corresponding EE was 68.31%, comparable with the predictive value of 68.30%. Physicochemical properties suggested the successful formation of inclusion complexes by CLEO displacing the internal water molecules. FTIR revealed changes in wavenumbers and peak intensity of inclusion complexes compared with CLEO, supporting CLEO entered in the cavity of  $\beta$ -CD. XRD spectroscopy reflected the transformation of crystal characteristics of inclusion complexes after complexation. The morphological characterizations observed by SEM exhibited that CLEO/ $\beta$ -CD-IC particles were smaller and formless agglomerates compared with physical mixtures. For TG analysis, disparate mass loss curves proved that the inclusion complexes had better thermal stability than that of free CLEO. CLEO/ $\beta$ -CD-IC supplied thermostability to CLEO compounds, and it was beneficial to expand the application of CLEO in the food, pharmaceutical, and daily chemical industries. CLEO/ $\beta$ -CD-IC can be a prospective novel material as a food preservative and pharmaceutical form based on the biological activities of CLEO. Consequently, the antimicrobial properties of CLEO/ $\beta$ -CD-IC should be investigated in further research.

**Author Contributions:** Conceptualization, Q.W.; methodology, Y.Y., C.W. and L.Z.; investigation, Y.Y. and C.W.; resources, X.Z.; writing—original draft preparation, Y.Y.; writing—review and editing, Q.W. and X.Z.; visualization, Y.Y.; supervision, Q.F.; project administration, Y.Y. All authors have read and agreed to the published version of the manuscript.

**Funding:** This research was supported by Doctor Launch Project of Yibin University (2020QH05) and Yibin High-end Innovation and Entrepreneurship Project (2021YGC03).

**Institutional Review Board Statement:** Not applicable.

**Informed Consent Statement:** Not applicable.

**Data Availability Statement:** Not applicable.

**Conflicts of Interest:** The authors declare no conflict of interest.

#### References

1. Zhao, X.; Yan, Y.; Zhou, W.H.; Feng, R.Z.; Shuai, Y.K.; Yang, L.; Liu, M.J.; He, X.Y.; Wei, Q. Transcriptome and metabolome reveal the accumulation of secondary metabolites in different varieties of *Cinnamomum longepaniculatum*. *BMC Plant Biol.* **2022**, *22*, 243. [[CrossRef](#)] [[PubMed](#)]
2. Huang, J.; Yang, L.; Zou, Y.; Luo, S.; Wang, X.; Liang, Y.; Du, Y.; Feng, R.; Wei, Q. Antibacterial activity and mechanism of three isomeric terpineols of *Cinnamomum longepaniculatum* leaf oil. *Folia Microbiol.* **2021**, *66*, 59–67. [[CrossRef](#)]
3. Yin, H.; Wang, C.; Yue, J.; Jiao, S.S.; Wang, X.H.; Jiang, L.L. Extraction of *Cinnamomum longepaniculatum* Essential Oil and Its Chemical Composition, Antioxidation and Antibacterial Properties. *Stored Proced.* **2020**, *20*, 183–191.
4. Li, L.; Li, Z.W.; Yin, Z.Q.; Wei, Q.; Jia, R.Y.; Zhou, L.J.; Xu, J.; Song, X.; Zhou, Y.; Du, Y.H.; et al. Antibacterial activity of leaf essential oil and its constituents from *Cinnamomum longepaniculatum*. *Int. J. Clin. Exp. Med.* **2014**, *7*, 1721–1727.
5. Du, Y.H.; Feng, R.Z.; Li, Q.; Wei, Q.; Yin, Z.Q.; Zhou, L.J.; Tao, C.; Jia, R.Y. Anti-inflammatory activity of leaf essential oil from *Cinnamomum longepaniculatum* (Gamble) N. Chao. *Int. J. Clin. Exp. Med.* **2014**, *7*, 5612–5620.
6. Su, Z.; Qin, Y.; Zhang, K.; Bi, Y.; Kong, F. Inclusion Complex of *Exocarpium Citri Grandis* Essential Oil with  $\beta$ -Cyclodextrin: Characterization, Stability, and Antioxidant Activity. *J. Food Sci.* **2019**, *84*, 1592–1599. [[CrossRef](#)]
7. Cao, C.; Wei, D.; Xu, L.; Hu, J.; Qi, J.; Zhou, Y. Characterization of tea tree essential oil and large-ring cyclodextrins (CD(9)-CD(22)) inclusion complex and evaluation of its thermal stability and volatility. *J. Sci. Food Agric.* **2021**, *101*, 2877–2883. [[CrossRef](#)]
8. Mura, P. Advantages of the combined use of cyclodextrins and nanocarriers in drug delivery: A review. *Int. J. Pharm.* **2020**, *579*, 119181. [[CrossRef](#)] [[PubMed](#)]
9. Hădărugă, N.G.; Szakal, R.N.; Chirilă, C.A.; Lukinich-Gruia, A.T.; Păunescu, V.; Muntean, C.; Rusu, G.; Bujancă, G.; Hădărugă, D.I. Complexation of Danube common nase (*Chondrostoma nasus* L.) oil by  $\beta$ -cyclodextrin and 2-hydroxypropyl- $\beta$ -cyclodextrin. *Food Chem.* **2020**, *303*, 125419. [[CrossRef](#)]
10. Marques, C.S.F.; Barreto, N.S.; Oliveira, S.S.C.; Santos, A.L.S.; Branquinha, M.H.; Sousa, D.P.; Castro, M.; Andrade, L.N.; Pereira, M.M.; Silva, C.F.D.; et al.  $\beta$ -Cyclodextrin/Isopentyl Caffeate Inclusion Complex: Synthesis, Characterization and Antileishmanial Activity. *Molecules* **2020**, *25*, 4181. [[CrossRef](#)]

11. Kringel, D.H.; Antunes, M.D.; Klein, B.; Crizel, R.L.; Wagner, R.; de Oliveira, R.P.; Dias, A.R.G.; Zavareze, E.D.R. Production, Characterization, and Stability of Orange or Eucalyptus Essential Oil/ $\beta$ -Cyclodextrin Inclusion Complex. *J. Food Sci.* **2017**, *82*, 2598–2605. [[CrossRef](#)]
12. Shrestha, M.; Ho, T.M.; Bhandari, B.R. Encapsulation of tea tree oil by amorphous beta-cyclodextrin powder. *Food Chem.* **2017**, *221*, 1474–1483. [[CrossRef](#)] [[PubMed](#)]
13. Cunha, F.V.M.; do Nascimento Caldas Trindade, G.; da Silva Azevedo, P.S.; Coêlho, A.G.; Braz, E.M.; Pereira de Sousa Neto, B.; de Rezende, D.C.; de Sousa, D.P.; de Assis Oliveira, F.; Nunes, L.C.C. Ethyl ferulate/ $\beta$ -cyclodextrin inclusion complex inhibits edema formation. *Mater. Sci. Eng. C Mater. Biol. Appl.* **2020**, *115*, 111057. [[CrossRef](#)] [[PubMed](#)]
14. Mu, K.; Jiang, K.; Wang, Y.; Zhao, Z.; Cang, S.; Bi, K.; Li, Q.; Liu, R. The Biological Fate of Pharmaceutical Excipient  $\beta$ -Cyclodextrin: Pharmacokinetics, Tissue Distribution, Excretion, and Metabolism of  $\beta$ -Cyclodextrin in Rats. *Molecules* **2022**, *27*, 1138. [[CrossRef](#)]
15. Lin, L.; Liao, X.; Li, C.; Abdel-Samie, M.A.; Siva, S.; Cui, H. Cold nitrogen plasma modified cuminaldehyde/ $\beta$ -cyclodextrin inclusion complex and its application in vegetable juices preservation. *Food Res. Int.* **2021**, *141*, 110132. [[CrossRef](#)]
16. Fuentes Campo, A.; Sancho, M.I.; Melo, G.; Dávila, Y.A.; Gasull, E. In vitro and in vivo inhibition of Hass avocado polyphenol oxidase enzymatic browning by paeonol,  $\beta$ -cyclodextrin, and paeonol: $\beta$ -cyclodextrin inclusion complex. *J. Biosci. Bioeng.* **2019**, *127*, 703–709. [[CrossRef](#)]
17. Kringel, D.H.; Lang, G.H.; Dias, Á.R.G.; Gandra, E.A.; Valente Gandra, T.K.; da Rosa Zavareze, E. Impact of encapsulated orange essential oil with  $\beta$ -cyclodextrin on technological, digestibility, sensory properties of wheat cakes as well as *Aspergillus flavus* spoilage. *J. Sci. Food Agric.* **2021**, *101*, 5599–5607. [[CrossRef](#)]
18. Hogenbom, J.; Istanbuli, M.; Faraone, N. Novel  $\beta$ -Cyclodextrin and Catnip Essential Oil Inclusion Complex and Its Tick Repellent Properties. *Molecules* **2021**, *26*, 7391. [[CrossRef](#)]
19. Hogenbom, J.; Jones, A.; Wang, H.V.; Pickett, L.J.; Faraone, N. Synthesis and Characterization of  $\beta$ -Cyclodextrin-Essential Oil Inclusion Complexes for Tick Repellent Development. *Polymers* **2021**, *13*, 1892. [[CrossRef](#)] [[PubMed](#)]
20. Marques, C.S.; Carvalho, S.G.; Bertoli, L.D.; Villanova, J.C.O.; Pinheiro, P.F.; Dos Santos, D.C.M.; Yoshida, M.I.; de Freitas, J.C.C.; Cipriano, D.F.; Bernardes, P.C.  $\beta$ -Cyclodextrin inclusion complexes with essential oils: Obtention, characterization, antimicrobial activity and potential application for food preservative sachets. *Food Res. Int.* **2019**, *119*, 499–509. [[CrossRef](#)] [[PubMed](#)]
21. Zhu, Y.; Yu, J.; Jiao, C.; Tong, J.; Zhang, L.; Chang, Y.; Sun, W.; Jin, Q.; Cai, Y. Optimization of quercetin extraction method in *Dendrobium officinale* by response surface methodology. *Heliyon* **2019**, *5*, e02374. [[CrossRef](#)] [[PubMed](#)]
22. Feng, C.H.; Drummond, L.; Sun, D.W.; Zhang, Z.-H. Evaluation of natural hog casings modified by surfactant solutions combined with lactic acid by response surface methodology. *LWT-Food Sci. Technol.* **2014**, *58*, 427–438. [[CrossRef](#)]
23. Feng, C.H. Optimizing Procedures of Ultrasound-Assisted Extraction of Waste Orange Peels by Response Surface Methodology. *Molecules* **2022**, *27*, 2268. [[CrossRef](#)] [[PubMed](#)]
24. Feng, C.H.; Sun, D.W. Optimisation of immersion vacuum cooling operation and quality of Irish cooked sausages by using response surface methodology. *Int. J. Food Sci. Technol.* **2014**, *49*, 1850–1858. [[CrossRef](#)]
25. Liu, Y.; Yin, Z.Q.; Wei, Q.; Jia, R.Y.; Fan, J.; Zhou, L.J.; Du, Y.H. Study on preparation process and stability of beta-cyclodextrin inclusion compound in volatile oil of *Cinnamomum longepaniculatum* leaves. *Zhongguo Zhong Yao Za Zhi* **2013**, *38*, 2105–2108.
26. Yang, Y.H.; Li, X.Z.; Zhang, S. Preparation methods and release kinetics of *Litsea cubeba* essential oil microcapsules. *RSC Adv.* **2018**, *8*, 29980–29987. [[CrossRef](#)]
27. Wu, J.; Zhang, J.; Yu, X.; Shu, Y.; Zhang, S.; Zhang, Y. Extraction optimization by using response surface methodology and purification of yellow pigment from *Gardenia jasminoides* var. *radicans* Makikno. *Food Sci. Nutr.* **2021**, *9*, 822–832. [[CrossRef](#)]
28. Wang, Y.; Yin, C.; Cheng, X.; Li, G.; Zhu, X.  $\beta$ -Cyclodextrin Inclusion Complex Containing *Litsea cubeba* Essential Oil: Preparation, Optimization, Physicochemical, and Antifungal Characterization. *Coatings* **2020**, *10*, 850. [[CrossRef](#)]
29. Bai, C.; Xu, P.; Qi, W.; Kong, Q.; Xiong, G. Preparation and characterization of a sustained-release bio-preservative based on  $\beta$ -cyclodextrin encapsulated eugenol. *Food Biosci.* **2021**, *42*, 101192. [[CrossRef](#)]
30. He, D.; Yan, L.; Hu, Y.; Wu, Q.; Wu, M.; Choi, J.I.; Tong, H. Optimization of Porphyran Extraction from *Pyropia yezoensis* by Response Surface Methodology and Its Lipid-Lowering Effects. *Mar. Drugs* **2021**, *19*, 53. [[CrossRef](#)] [[PubMed](#)]
31. Torres-Alvarez, C.; Castillo, S.; Sánchez-García, E.; Aguilera González, C.; Galindo-Rodríguez, S.A.; Gabaldón-Hernández, J.A.; Báez-González, J.G. Inclusion Complexes of Concentrated Orange Oils and  $\beta$ -Cyclodextrin: Physicochemical and Biological Characterizations. *Molecules* **2020**, *25*, 5109. [[CrossRef](#)] [[PubMed](#)]
32. Petrović, G.M.; Stojanović, G.S.; Radulović, N.S. Encapsulation of cinnamon oil in  $\beta$ -cyclodextrin. *J. Med. Plants Res.* **2010**, *4*, 1382–1390.
33. Ma, S.; Zhao, Z.; Liu, P. Optimization of preparation process of  $\beta$ -cyclodextrin inclusion compound of clove essential oil and evaluation of heat stability and antioxidant activities in vitro. *J. Food Meas. Charact.* **2018**, *12*, 2057–2067. [[CrossRef](#)]
34. Li, H.; Chang, S.L.; Chang, T.R.; You, Y.; Zhao, B. Inclusion complexes of cannabidiol with  $\beta$ -cyclodextrin and its derivative: Physicochemical properties, water solubility, and antioxidant activity. *J. Mol. Liq.* **2021**, *334*, 116070. [[CrossRef](#)]
35. Sampath, S.; Subramani, S.; Janardhanam, S.; Subramani, P.; Yuvaraj, A.; Chellan, R. Bioactive compound 1,8-Cineole selectively induces G2/M arrest in A431 cells through the upregulation of the p53 signaling pathway and molecular docking studies. *Phytomedicine* **2018**, *46*, 57–68. [[CrossRef](#)]
36. Biernacka, M.; Ilyich, T.; Zavodnik, I.; Patecz, B.; Stepniak, A. Studies of the Formation and Stability of Ezetimibe-Cyclodextrin Inclusion Complexes. *Int. J. Mol. Sci.* **2021**, *23*, 455. [[CrossRef](#)]

37. Mashaqbeh, H.; Obaidat, R.; Al-Shar'i, N. Evaluation and Characterization of Curcumin- $\beta$ -Cyclodextrin and Cyclodextrin-Based Nanosponge Inclusion Complexation. *Polymers* **2021**, *13*, 4073. [[CrossRef](#)]
38. Franco, P.; De Marco, I. Formation of Rutin- $\beta$ -Cyclodextrin Inclusion Complexes by Supercritical Antisolvent Precipitation. *Polymers* **2021**, *13*, 246. [[CrossRef](#)]
39. Gao, S.; Liu, Y.; Jiang, J.; Ji, Q.; Ye, F. Physicochemical properties and fungicidal activity of inclusion complexes of fungicide chlorothalonil with  $\beta$ -cyclodextrin and hydroxypropyl- $\beta$ -cyclodextrin. *J. Mol. Liq.* **2019**, *293*, 111513. [[CrossRef](#)]
40. Sbârcea, L.; Udrescu, L.; Ledeti, I.; Szabadai, Z.; Fuliş, A.; Sbârcea, C.  $\beta$ -Cyclodextrin inclusion complexes of lisinopril and zofenopril. *J. Therm. Anal. Calorim.* **2016**, *123*, 2377–2390. [[CrossRef](#)]
41. Zhang, W.; Li, X.; Yu, T.; Yuan, L.; Rao, G.; Li, D.; Mu, C. Preparation, physicochemical characterization and release behavior of the inclusion complex of trans-anethole and  $\beta$ -cyclodextrin. *Food Res. Int.* **2015**, *74*, 55–62. [[CrossRef](#)]
42. Tao, F.; Hill, L.E.; Peng, Y.; Gomes, C.L. Synthesis and characterization of  $\beta$ -cyclodextrin inclusion complexes of thymol and thyme oil for antimicrobial delivery applications. *LWT-Food Sci. Technol.* **2014**, *59*, 247–255. [[CrossRef](#)]
43. Fauziah, C.I.; Zaibunnisa, A.H.; Osman, H.; Aida, W. Thermal Analysis and Surface Morphology Study of Cholesterol:  $\beta$ -Cyclodextrin Inclusion Complex. *Adv. Mater. Res.* **2013**, *812*, 221–225. [[CrossRef](#)]
44. Oliveira Brito Pereira Bezerra Martins, A.; Wanderley, A.G.; Alcântara, I.S.; Rodrigues, L.B.; Cesário, F.; Correia de Oliveira, M.R.; Castro, F.F.E.; Albuquerque, T.R.; da Silva, M.S.A.; Ribeiro-Filho, J.; et al. Anti-Inflammatory and Physicochemical Characterization of the *Croton Rhamnifolioides* Essential Oil Inclusion Complex in  $\beta$ -Cyclodextrin. *Biology* **2020**, *9*, 114. [[CrossRef](#)] [[PubMed](#)]
45. Dos Passos Menezes, P.; de Oliveira Araujo, F.; Andrade, T.A.; Trindade, I.A.S.; de Araujo-Filho, H.G.; de Souza Siqueira Quintans, J.; Quintans-Junior, L.J.; Menezes, L.R.A.; de Almeida, R.N.; Braga, R.M.; et al. Physicochemical Characterization and Antinociceptive Effect of  $\beta$ -cyclodextrin/*Lippia pedunculosa* Essential Oil in Mice. *Curr. Top. Med. Chem.* **2018**, *18*, 797–807. [[CrossRef](#)]